

# LONGITUDINAL PERFORMANCE WITH HIGH-DENSITY BEAMS FOR THE LHC IN THE CERN PS

H. Damerou\*, S. Hancock, M. Schokker, CERN, Geneva, Switzerland

## Abstract

As one of the pre-injectors for the Large Hadron Collider, the CERN Proton Synchrotron must reliably deliver beams in a wide range of parameters. The large variety of bunch spacings from 25 to 150 ns at extraction requires the acceleration of small, high-density bunches as well as highly intense ones. Above a threshold bunch density, longitudinal coupled-bunch instabilities are observed after transition crossing and the main accelerating cavities have been identified as part of the impedance driving them. Transient beam loading causes asymmetries of the various bunch splittings used to establish the required bunch spacing, compromising beam quality at the head of the bunch train delivered. Recent measurements of longitudinal limitations of beams for the LHC are presented, together with possible cures and options for future hardware improvements.

## INTRODUCTION

The optimum bunch spacing in the Large Hadron Collider (LHC), especially during the commissioning phase, is determined by a large set of constraints from the machine itself, as well as from the experiments. Hence, the accelerators in the injector chain of the LHC must be flexible to provide bunches spaced by 25, 50, 75 or 150 ns. The 150 ns variant had originally not been foreseen. Following a request by the LHC experiments, it has been set-up in 2010 for the first time. It is important that the bunch parameters at injection into the LHC are independent from bunch spacing.

The major part of the preparation of the different variants of LHC-type beams is performed by radio frequency (RF) manipulations already in the Proton Synchrotron (PS). In all cases, up to six bunches from the PS Booster (PSB) are injected into RF buckets at the 7<sup>th</sup> harmonic ( $h = 7$ ) of the revolution frequency,  $f_{rev}$ . One bucket remains empty to provide a gap for the PS extraction kicker. The up to  $\tau_{batch} = 1.8 \mu s$  long batch sent to the Super Proton Synchrotron (SPS) may thus be filled with  $\tau_{batch}/\tau_{bs}$  bunches spaced by  $\tau_{bs}$ . The different variants of the LHC-type beams are produced by combinations of triple and double bunch splittings on both injection and extraction plateaus (Table 1). For these manipulations the PS is equipped with sets of cavities covering frequencies of 2.8–10 MHz (ferrite-loaded, tunable), 13.3 MHz, 20 MHz, 40 MHz and 80 MHz. Additional cavities at 200 MHz are used for controlled blow-up of the longitudinal emittance. The labels LHC25ns, LHC50ns, etc. are used throughout

Table 1: Longitudinal Manipulations for the Different Variants of Nominal LHC-type Beams [1, 2]. Each bunch (b) is split in two (2-split) or three (3-split) parts.

LHC25ns	LHC50ns	LHC75ns	LHC150ns
Inject 6 bunches on harmonic $h = 7$			
Flat-bottom RF manipulation			
Controlled emittance blow-up to match splitting			
3-split	3-split	2-split	2-split
$h = 7, 14, 21$		$h = 7, 14$	
Blow-up for transition			
Acceleration			
18b, $h = 21$		12b, $h = 14$	
Blow-up			
Intensity and longitudinal emittance per bunch:			
$5.2 \cdot 10^{11}$	$2.6 \cdot 10^{11}$	$2.6 \cdot 10^{11}$	$1.3 \cdot 10^{11}$
1.3 eVs	0.65 eVs	0.65 eVs	0.33 eVs
Total intensity for $N_b = 1.3 \cdot 10^{11}$ ppb at extraction:			
$9.4 \cdot 10^{12}$	$4.7 \cdot 10^{12}$	$3.1 \cdot 10^{12}$	$1.6 \cdot 10^{12}$
1 <sup>st</sup> RF manipulation on flat-top			
2-split	2-split	2-split	
$h = 21, 42$		$h = 14, 28$	
2 <sup>nd</sup> RF manipulation on flat-top			
2-split	Rebucket	Rebucket	Rebucket
$h = 42, 84$		$h = 28, 84$	$h = 14, 84$
Bunch shortening on $h = 84$ , final bunch pattern:			
72b, 25 ns	36b, 50 ns	24b, 75 ns	12b, 150 ns

this paper to indicate the beam type according to its bunch spacing at extraction, which differs from the bunch spacing during acceleration in most cases.

As each bunch at extraction to the SPS should nominally contain  $N_b = 1.3 \cdot 10^{11}$  ppb within a longitudinal emittance of  $\varepsilon_l = 0.35$  eVs ( $2\sigma$ ), the total intensity of the beam accelerated in the PS varies from  $1.6 \cdot 10^{12}$  ppp (150 ns bunch spacing) to  $9.4 \cdot 10^{12}$  ppp (25 ns). The average longitudinal density,  $N_b/\varepsilon_l = 3.7 \cdot 10^{11}$  p/eVs, during the last part of acceleration and on the flat-top is however identical for all different species. Since the harmonic number during acceleration is the same for LHC25ns/LHC50ns ( $h = 21$ ) and LHC75ns/LHC150ns ( $h = 14$ ), this allows direct comparison of beams with the same longitudinal density but very different total intensity. In the PS, the maximum intensity with LHC-type beams remains well below the intensity of beams accelerated for fixed-target experiments ( $> 3 \cdot 10^{13}$  ppp), but the latter beams are much less dense.

\* heiko.damerou@cern.ch

Measurements comparing the longitudinal limitations of LHC25ns/LHC50ns beams and the corresponding driving impedance sources, as far as they have been identified, are presented in the first part of the paper. Key ingredients to achieve bunch intensities well beyond nominal intensity of  $1.3 \cdot 10^{11}$  ppb are introduced. Thereafter, the longitudinal performance with LHC75ns and the new beam variant with 150 ns bunch spacing (LHC150ns) are reported. Finally, ongoing and possible future upgrades of the feedback systems are discussed.

## PERFORMANCE LIMITATIONS WITH 25 AND 50 NS BUNCH SPACING

Comparing longitudinal beam stability of the LHC-type beams with 25 and 50 ns bunch spacing at extraction is motivated by the fact that both beam types are very similar during acceleration (see Table 1). In both cases, 18 bunches are accelerated at  $h = 21$ . The longitudinal density is the same as well, but intensity and longitudinal emittance of the 50 ns variant are twice smaller.

### *Coupled-bunch Instabilities During Acceleration*

As coupled-bunch (CB) oscillations usually start after transition crossing, mountain range data were recorded every 70 ms starting from 100 ms after transition crossing, when the final  $\varepsilon_l$  is reached for LHC25ns and LHC50ns beams (the magnetic cycle for the LHC50ns beam is 1.2 s shorter due to single-batch transfer from the PSB [3]). The dipole motion of each bunch is extracted from the center position of a Gaussian function fitted to each bunch of each turn recorded. A second fit of a sinusoidal function to the motion of the bunch center results in oscillation amplitude, phase and frequency, the latter being the synchrotron frequency. A discrete Fourier transform converts these oscillation amplitudes and phases per bunch to amplitudes and phases per mode, the mode spectrum [4]. This analysis technique is superior to measurements in frequency domain since the bunches only cover 6/7 of the circumference. Spurious  $f_{\text{rev}}$  lines due to this filling pattern are removed as only bunches are analyzed. However, the mode numbers with respect to the batch,  $n_{\text{batch}}$  do not directly correspond to  $f_{\text{rev}}$  harmonics, but each mode number  $n_{\text{batch}}$  results in a spectrum of  $f_{\text{rev}}$  lines, with the lines close to  $7/6 n_{\text{batch}} f_{\text{rev}}$  at maximum amplitudes.

Figures 1 and 2 show the evolution of the mode spectra for LHC25ns and LHC50ns beams during acceleration. Though the total intensity differs by a factor two, the mode pattern and oscillation amplitudes are very similar, suggesting a scaling proportional to longitudinal density,  $N_b/\varepsilon_l$  rather than intensity.

Moreover, the form of the spectrum remains unchanged during acceleration. The modes  $n_{\text{batch}} = 1, 2$  and  $16, 17$ , those close to the RF harmonic, are strongest. No individual mode, which peaks at a certain moment during acceleration and then disappears again, is observed. This points to

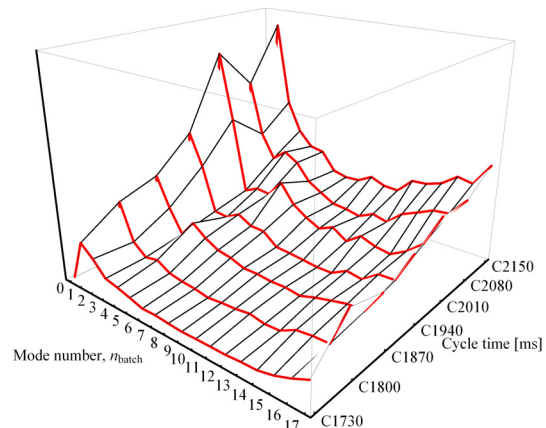


Figure 1: LHC25ns: CB mode spectrum during acceleration averaged over ten cycles for each measurement time.

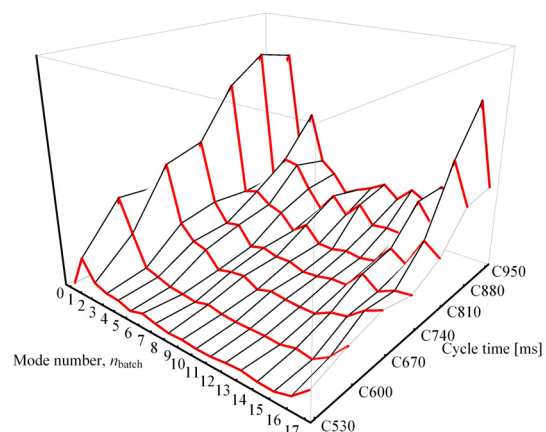


Figure 2: LHC50ns: Development of the CB mode spectrum during acceleration. Same vertical scale (arbitrary units) as Fig. 1.

a driving impedance with a relative bandwidth of at least 1.4% (the  $f_{\text{rev}}$  swing after transition crossing, which is given by  $\simeq 1 - \sqrt{1 - 1/\gamma_{\text{tr}}^2}$ ,  $\gamma_{\text{tr}} = 6.1$ ).

### *Coupled-bunch Instabilities on the Flat-top*

After arrival on the flat-top, the batch is normally synchronized with the SPS on  $h = 1$ , before the splittings start. For a symmetric splitting of all bunches, CB oscillations must not be present at this point. To allow for easier analysis of CB instabilities on the flat-top, the splittings were disabled and the beam kept at low RF voltage at  $h = 21$  for about 150 ms until extraction. The RF voltages of 10 kV (LHC25ns) and 20 kV (LHC50ns) correspond to the values at the start of the bunch splittings. Figure 3 illustrates the slowly growing oscillations during the flat-top with low voltage at  $h = 21$ . Dipole oscillations develop especially at the tail of the batch. The same mode analysis procedure described above has been applied to the well developed CB oscillations close to extraction. The mode spectra, averaged over ten cycles, are shown in Fig. 4. Again,

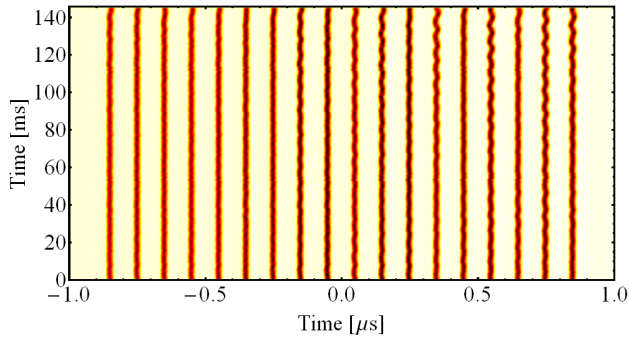


Figure 3: Mountain range density plot of a batch of 18 bunches kept at  $h = 21$  with 20 kV (the initial condition for the splitting  $h = 21 \rightarrow 42$ ) along the flat top (LHC50ns).

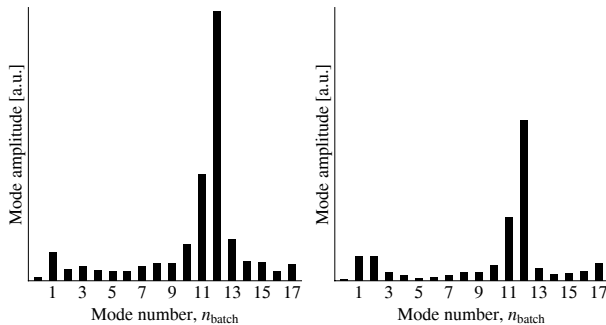


Figure 4: Comparison of the CB mode spectrum on the flat-top of LHC25ns (left) and LHC50ns (right) beams. In both cases a batch of 18 bunches is kept at low voltage on  $h = 21$  until extraction. The vertical scale of both plots is identical.

LHC25ns and LHC50ns beams feature very similar mode spectra despite their difference in total intensity and longitudinal emittance, confirming the aforementioned scaling with longitudinal density.

The strongest modes present on the flat-top are  $n_{\text{batch}} = 11$  and 12, very different from the dominant modes observed during acceleration. This suggests that the driving impedance changes. Indeed the configuration of the ten 2.8 – 10 MHz cavities is modified after the arrival on the flat-top. During acceleration, all 10 MHz cavities are active, close to full voltage (20 kV per cavity) and with their gaps open. To achieve the moderate RF voltages before the splitting on the flat-top in a well controlled fashion, eight of ten cavities are switched off in a sequence leaving only two active cavities. The unused cavities remain tuned close to the RF harmonic but are short-circuited by a gap relay.

It was found that the residual impedance of those short-circuited, inactive cavities represents an important part of the impedance driving the CB instabilities on the flat-top. Two passive impedance reductions are described below.

Results from recent beam tests pushing the intensity of the LHC25ns and LHC50ns beams towards ultimate, indicate that intensities up to almost  $1.9 \cdot 10^{11}$  protons per

extracted bunch within a longitudinal emittance slightly above  $\varepsilon_l = 0.38$  eVs can be obtained for both bunch spacings. In addition to the passive cures, active CB feedback on  $h = 19/20$ , mainly damping the dominant modes  $n = 1, 2$  and 16, 17, significantly improves stability during acceleration. Fast controlled longitudinal blow-up directly after transition crossing avoids a too fast growth of CB instabilities in the case of LHC25ns.

### Detuning Unused RF Cavities

The ten ferrite-loaded cavities of the main acceleration system in the PS can be electrically tuned in three groups (tuning current loops are in series) from 2.8 – 10 MHz. On the flat-top, cavities were originally short-circuited only, but the tuning current was kept unchanged as if they were still operational on  $h = 21$  or  $h = 14$ . This was found to contribute to the excitation of CB instabilities, hence a new tuning scheme was implemented. At the moment the last cavity of a tuning group is programmed to zero, the group is rapidly tuned to a parking frequency of 3.1 MHz ( $h = 6.5$ ), the lowest possible in-between two  $f_{\text{rev}}$  harmonics.

### Gap Relays

Each of the ferrite-loaded cavities consists of two  $\lambda/4$ -resonators, each of them with an acceleration gap, connected in parallel by two coaxial bars and the tuning loop [5]. Originally, both gaps were short-circuited, but in 1991, shortly after the significant impedance reduction by direct RF feedback [6], the second gap relay was removed to reduce maintenance costs. Following the analysis of the instability observations presented above, four of the ten cavities have been re-equipped with a second gap relay. The beam induced voltage along an acceleration cycle (fixed-target SPS) measured across the left and right gaps is shown in Fig. 5. The asymmetry of the induced volt-

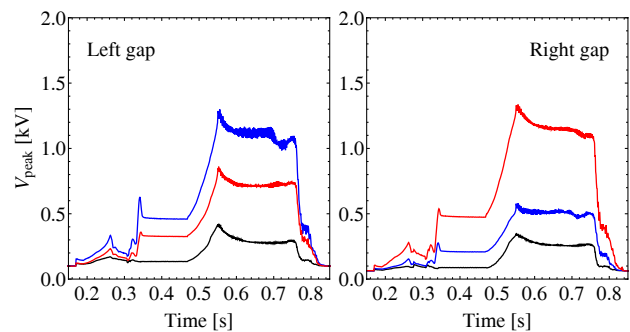


Figure 5: Beam induced voltage (cavity in straight section 46) measured on left and right accelerating gaps. Black: both gap relays closed; red: left relay closed only; blue: right relay closed only.

age is different from cavity to cavity, but a reduction of the voltage by more than a factor of two, due to the second gap

relay is observed on average. The remaining cavities will thus be equipped with a second gap relay for the 2011 run.

### Transient Beam-loading

At intensities beyond nominal, transient beam loading compromises the longitudinal quality of the batch since the symmetry of the bunch splittings becomes dependent on the position within the batch, resulting in unequal bunch intensities and emittances. Figure. 6 illustrates this effect for an LHC50ns beam at an intensity of  $1.9 \cdot 10^{11}$  ppb (50 % above nominal). At extraction an intensity variation from

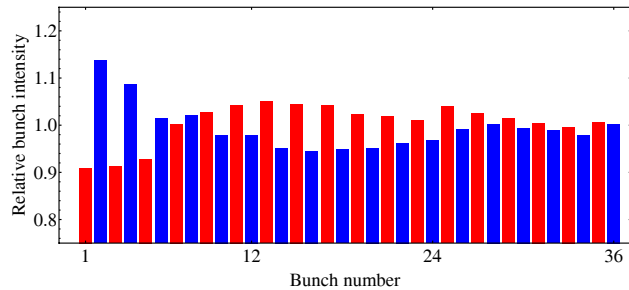


Figure 6: Relative bunch intensity at extraction versus position within the batch (averaged over ten cycles, LHC50ns,  $1.9 \cdot 10^{11}$  ppb).

bunch to bunch, caused by the bunch splitting  $h = 21 \rightarrow 42$ , is clearly visible, especially at the head of the batch.

This effect is caused by transient beam loading. The relative phase of the cavity return signals ( $h = 21/42$ ) in the middle of the splitting is plotted for various batch lengths in Fig. 7. For these fast measurements, both cavity re-

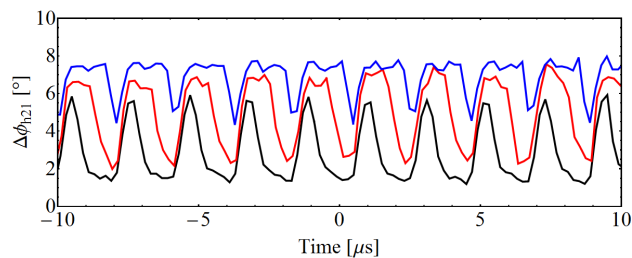


Figure 7: Phase error between 10 and 20 MHz versus time (LHC50ns,  $1.9 \cdot 10^{11}$  ppb, constant offsets removed). The vertical scale is in degrees with respect to the lower harmonic  $h = 21$ . The batch length is 12 (black), 24 (red) or 36 bunches (blue), corresponding to  $2/7$ ,  $4/7$  and  $6/7$  of the circumference. The periodicity is  $1/f_{\text{rev}} = 2.1 \mu\text{s}$ .

turn signals were sampled at 2.5 GS/s and the phase calculated from sinusoidal fits to 200 ns long intervals of the sampled traces. The amplitude of the phase oscillations caused by transient beam loading is about  $4^\circ$ , similar to previous estimations based on the asymmetry of the bunch shape in the  $h = 21 + h = 42$  double-harmonic RF system [7]. Due to insufficient time resolution of the measure-

ment, the phase oscillations appear smaller in the 36 bunch case. Comparing forward and return phases of the cavities at  $h = 21$ , suggests that these cavities are more prone to transient beam loading than the 20 MHz cavity ( $h = 42$ ).

### 75 NS BUNCH SPACING

For the LHC75ns beam at nominal intensity, only weak CB oscillations are observed during acceleration from transition crossing to flat-top. On the flat-top however, the LHC75ns beam exhibits similar stability problems as reported above for the 25 ns and 50 ns variants. The measured CB mode spectrum is shown in Fig. 8, again disabling the RF manipulations on the flat-top and keeping the beam at low RF voltage on  $h = 14$  (20 kV). Compared

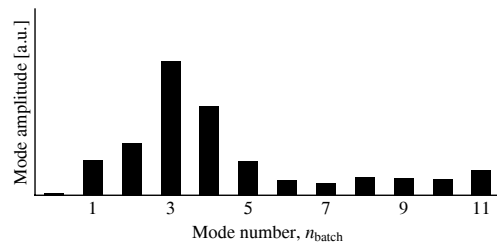


Figure 8: CB mode spectrum of oscillations on the flat-top of the beam for 75 ns bunch spacing. The RF voltage of 20 kV is generated by a single cavities while the other nine cavities are short-circuited by a gap relay.

to LHC25ns and LHC50ns (Fig. 4), the mode spectrum is shifted to lower mode numbers which may be due to the lower RF harmonic ( $h = 14$  instead of  $h = 21$ ). Though no tests to push the LHC75ns beam to highest possible intensities per bunch have been performed yet, it is expected that this beam will also benefit from the recently introduced improvements for the other LHC beam variants.

### 150 NS BUNCH SPACING

A beam variant with 150 ns bunch spacing has been set-up for the first time in 2010 and is used now in the LHC. Up to 12 bunches are ejected to the SPS, and a total intensity of only  $1.6 \cdot 10^{12}$  ppb is accelerated for nominal intensity per bunch. However, as the longitudinal density during acceleration must be as high as with the other beams for LHC, a longitudinal emittance below  $\varepsilon_l = 0.35$  eVs must be well preserved. With such a small emittance, a zero-mode ( $n = 1$ ) quadrupolar instability is triggered at transition. Damping of this mode is achieved by a slow feedback, the so-called Hereward damping, modulating the voltage program of the accelerating cavities.

### Quadrupole Coupled-bunch Instabilities

After transition crossing, slowly growing quadrupolar ( $m = 2$ ,  $n_{\text{batch}} = 1$ ) CB instabilities (bunch length oscillations) are observed (Fig. 9). The high frequency (40/80 MHz) cavities [8] have been easily identified as

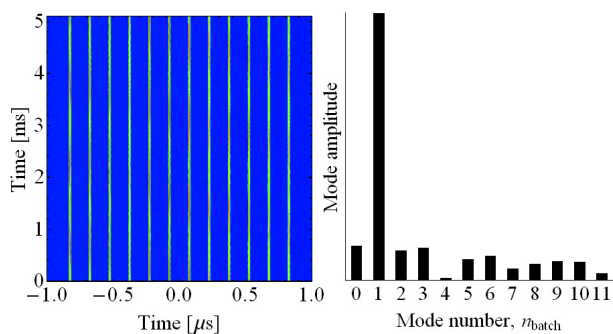


Figure 9: Quadrupole CB oscillation of the LHC150ns beam. Left: Mountain range density plot; right: Resulting quadrupole mode spectrum.

sources exciting those instabilities by opening and short-circuiting their gaps. Figure 10 compares two cases: all 40/80 MHz cavities closed with their gap short-circuits and all open (with active feedback). Obviously, keeping the

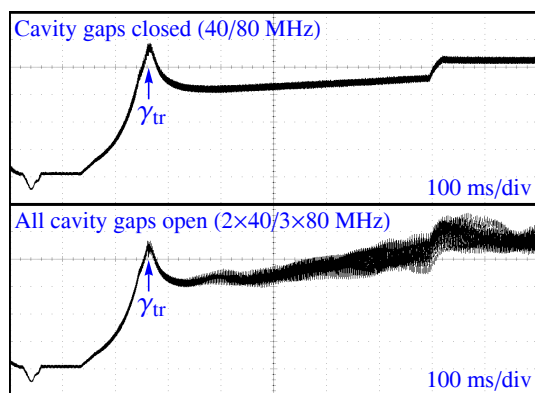


Figure 10: Peak detected beam signal from injection to the flat-top. With the cavity gaps open (active feedback for impedance reduction only), the beam is longitudinally unstable after transition crossing.

cavities short-circuited would be best, but one 40 MHz and two 80 MHz cavities are required for re-bucketing and bunch rotation prior to ejection. The pneumatic short-circuit opens too slowly to be switched during the acceleration cycle.

First beam tests have demonstrated that the quadrupolar CB oscillations can be kept under control with a feedback system working in frequency domain. The spectral components of the beam signal on  $h = 12$  and  $13$  are demodulated and then filtered to remove the revolution frequency harmonics, keeping only sidebands at  $n = 1, 2, \dots$  times the synchrotron frequency. The filtered base-band signal is then mixed back to the original harmonic (12/13) and fed as a correction signal to two RF cavities serving as feedback kickers.

No change of the CB mode spectrum is observed on the

flat-top with the LHC150ns beam as the RF voltage on  $h = 14$  stays at its maximum value of 200 kV (no cavity short-circuited), and the beam is directly handed over to  $h = 84$ .

## CONCLUSION

Results from the CB oscillations analysis for LHC25ns and LHC50ns beams have confirmed that the 10 MHz cavities, even when short-circuited, significantly contribute to the longitudinal impedance driving these instabilities. Unused cavities are now tuned to a parking frequency and a second gap relay will be installed on all cavities. With optimized feedback settings, an intensity of almost  $1.9 \cdot 10^{11}$  ppb has been achieved within bunch length and longitudinal emittance close to those at nominal intensity. However, the bunch-to-bunch intensity spread increases, especially at the head of the batch.

With the new LHC150ns beam, longitudinal stability problems already occur with the nominal intensity of  $1.3 \cdot 10^{11}$  ppb after transition crossing. The residual impedance of the 40/80 MHz cavities has been identified as main driving source. First tests with the existing CB feedback were successful, but incompatible with the normal operation.

A new feedback board to improve the performance and flexibility of 1-turn and CB feedbacks is being developed. Comb filter type feedbacks for the 40/80 MHz cavities based on the same electronics are also being considered.

The authors are grateful to Elena Shaposhnikova and Wolfgang Höfle.

## REFERENCES

- [1] R. Garoby, "Multiple Splitting in the PS: Results and Plans", LHC Workshop, Chamonix, France, 2001, pp. 32-36
- [2] R. Garoby, "A Non-adiabatic Procedure in the PS to Supply the Nominal Proton Bunches for LHC into 200 MHz RF Buckets in SPS", PS/RF/Note 93-17, CERN, Geneva, Switzerland, 1993
- [3] A. Blas, C. Carli, A. Findlay, R. Garoby, S. Hancock, K. Hanke, B. Mikulec, M. Schokker, "Studies of Single-batch Transfer of LHC-type Beams Between the CERN PS Booster and the PS", PAC'09, Vancouver, Canada, 2009
- [4] H. Damerau, S. Hancock, M. Mehler, C. Rossi, E. Shaposhnikova, J. Tückmantel, J.-L. Vallet, "Longitudinal Coupled-bunch Instabilities in the CERN PS", PAC'07, Albuquerque, New Mexico, USA, 2007, p. 4180-4182
- [5] H.-Ch. Grassmann, R. Jankovsky, W. Pirkel, "New RF System for the 28 GeV Proton Synchrotron at CERN", Siemens Review XLIV (1977), No. 4, pp. 164-170
- [6] R. Garoby, J. Jamsek, P. Konrad, G. Lobeau, G. Nassibian, "RF System for High Beam Intensity Acceleration in the CERN PS", PAC'89, Chicago, Illinois, 1989, pp. 135-137
- [7] C. M. Bhat, F. Caspers, H. Damerau, S. Hancock, E. Mahner, F. Zimmermann, "Stabilizing Effect of a Double-harmonic RF System in the CERN PS", PAC'09, Vancouver, Canada, 2009
- [8] M. Benedikt, A. Blas, J. Borborough et al., "The PS Complex as Proton Pre-Injector for the LHC - Design and Implementation Report", CERN 2000-03, CERN, Geneva, Switzerland, pp. 42-48